Atmos. Meas. Tech. Discuss., 4, 6615–6642, 2011
www.atmos-meas-tech-discuss.net/4/6615/2011/
doi:10.5194/amtd-4-6615-2011

Atmospheric
Measurement
Techniques
Discussions

Long term NO_2 measurements in Hong Kong using LED based Long Path Differential Optical Absorption Spectroscopy

K. L. Chan[1], D. Pöhler[2], G. Kuhlmann[1], A. Hartl[1], U. Platt[2], and M. O. Wenig[1]

[1]School of Energy and Environment, City University of Hong Kong, China
[2]Institute for Environmental Physics, Heidelberg University, Germany

Received: 12 August 2011 – Accepted: 19 October 2011 – Published: 2 November 2011

Correspondence to: K. L. Chan (kalokchan7@student.cityu.edu.hk)

Published by Copernicus Publications on behalf of the European Geosciences Union.

Abstract

In this study we present the first long term measurements of atmospheric nitrogen dioxide (NO_2) using a LED based Long Path Differential Optical Absorption Spectroscopy (LP-DOAS) instrument. This instrument is measuring continuously in Hong Kong since December 2009, first in a setup with a 550 m absorption path and then with a 3820 m path at about 30 m to 50 m above street level. The instrument is using a high power blue light LED with peak intensity at 450 nm coupled into the telescope using a Y-fibre bundle. The LP-DOAS instrument measures NO_2 concentrations in the Kowloon Tong and Mong Kok district of Hong Kong and we compare the measurement results to concentrations reported by monitoring stations operated by the Hong Kong Environmental Protection Department in that area. Hourly averages of coinciding measurements are in reasonable agreement ($R = 0.74$). Furthermore, we used the long-term data set to validate the Ozone Monitoring Instrument (OMI) NO_2 data product. Monthly averaged LP-DOAS and OMI measurements correlate well ($R = 0.84$) when comparing the data for the OMI overpass time. We analyzed weekly patterns in both data sets and found that the LP-DOAS detects a clear weekly cycle with a reduction on weekends during rush hour peaks, whereas OMI is not able to observe this weekly cycle due to its fix overpass time.

1 Introduction

Nitrogen dioxide (NO_2) is one of the most important trace gases in the atmosphere with impact on atmospheric chemical processes and public health. Nitrogen oxides (NO_x), defined as the sum of nitrogen oxide (NO) and nitrogen dioxide (NO_2), participate in the catalytic destruction of ozone (O_3) in the stratosphere (Crutzen, 1970), while being a catalyst for ozone formation in the troposphere. Acid rain caused by NO_x is known to have adverse impact on forest, freshwater and soil, harming insects and aquatic life-forms, as well as causing damage to buildings and having a negative impact on public health. NO_2 may also play an important role in radiative warming of the earth's atmosphere (Solomon et al., 1999). Besides natural sources and biomass burning, fossil fuel combustion is estimated to contribute about 50 % to the global NO_x emission (Lee et al., 1997). In Hong Kong, the atmospheric NO_2 levels are strongly related to traffic volume (Lau et al., 2008) and power generation. Due to prevailing easterlies in Hong Kong, most of the power plants are built in the western part of Hong Kong to minimize the impact on the populated area. As in most metropolitan areas the NO_2 concentration level varies rapidly with time. Having an accurate NO_2 measurement with high temporal resolution is very important for air quality monitoring and pollution management.

Differential Optical Absorption Spectroscopy (DOAS), introduced by Platt et al. (1979), is a spectroscopic measurement technique which has been used successfully for decades for atmospheric trace gas retrieval. DOAS allows direct and sensitive detection of multiple trace gases simultaneously without influencing their chemical interactions. It uses distinct narrow band absorption structures of the different trace gases for quantitative detection and concentration estimation by separating them from the broad band parts caused mainly by atmospheric scattering and broad band absorption.

In this paper, details of our experimental setup of the fibre long path DOAS instrument with LED are presented. The data are automatically analyzed for NO_2 and published on our website in near real time. The LP-DOAS NO_2 measurements are compared to the concentrations measured by a nearby monitoring station which is operated by the Hong Kong Environmental Protection Department (EPD), as well as the NO_2 data measured by the Ozone Monitoring Instrument (OMI) on board NASA's Aura satellite.

2 Experimental setup and retrieval procedure

A sketch of the fibre LP-DOAS instrument setup is shown in Fig. 1. The LP-DOAS setup consists of a blue LED light source, a telescope acting as sending and receiving unit and an array of retro reflectors (2–7 single quartz glass prisms each 63 mm in diameter) at the other end of the absorption path. Optical fibers were used as transmitter for the light between light source and telescope and telescope and spectrograph, respectively (Merten et al., 2011). The fibers are connected in a Y-bundle (5 m length) with six 200 µm transmitting fibers (NA = 0.22) from the LED light source surrounding one 200 µm receiving fiber which is connected to the spectrometer. The high power LED is placed on a heat sink in order to stabilize the temperature. The light of the high power blue LED (CREE XR-E 7090 royal blue, 440–455 nm FWHM) with ∼600 mW radiant flux (at 700 mA) is collimated into the six fibres by a quartz glass lens with f = 25 mm. The combined Y-fiber end is placed close to the focal point of the telescope's main mirror of 20 cm diameter and 60 cm focal length and thus produces an almost parallel light beam. Two stepper motors allow precise adjustment of the telescope to the retro reflector array. Light coming back from the retro reflector array is collected by the receiving fibre and redirected to a Triax 320 spectrometer (Jobin Yvon, f-number = 4.0, 1200 l mm^{-1} grating and blaze 500 nm, f = 320 mm, wavelength range from 400 to 462 nm, thermostated to 30 °C). The detector is a HMT (Hoffmann Messtechnik) 1024 pixel photodiode array detector (with Hamamatsu S3904–1024 chip) temperature stabilized to 0 °C. The 200 µm fibre acts as entrance slit, resulting in a spectral resolution of 0.4 nm (FWHM). To guarantee a homogeneous illumination of the spectrometer a mode mixer is applied by bending and vibrating the fibre (Stutz and Platt, 1997).

In this study, two measurement setups were realized (see Fig. 2). Setup 1 was operational from December 2009 till November 2010 with a total absorption path of 550 m across the campus of the City University of Hong Kong (CityU) campus. Both the instrument and the reflector were located on top of university buildings at opposite ends of the campus. Setup 2 is operational since December 2010 with a total absorption path of 3820 m. The instrument is located at CityU and the retro reflector is installed at the 22nd floor of the Langham Place Hotel at 70 m height in the center of Kowloon. The measurement path covers the University campus, residential areas and areas with heavy traffic.

A measurement sequence starts with taking an atmospheric spectrum with a maximum of 10 scans followed by 10 scans of the LED reference spectrum. The LED reference spectrum is taken by using a shortcut system consisting of an aluminum diffuser plate that is put several millimeters in front of the fibre bundle. The narrow band structures of the LED reference spectra are used to account for changes in the detector and the LED itself in order to improve the quality of the DOAS fit. Afterwards an atmospheric background spectrum is taken by blocking the LED using a shutter with a fixed integration time of 1 s and 1 scan. A full measurement sequence takes between 30 s and 60 s depending on visibility conditions. For the LP-DOAS measurement and data evaluation the software DOASIS (Kraus, 2005) is used.

The calibration of the spectrograph is performed using the emission lines of a Mercury lamp and a Xenon glow lamp. The Mercury emission line at 435.84 nm is used to convolve the literature reference spectra to the instrument resolution. The measured data are evaluated by the DOASIS software. All spectra are corrected for offset, dark current and background before the DOAS fit. The measurement spectrum is then divided by the LED reference spectrum before taking the logarithm. In order to remove the broad band structures from the spectrum, a high pass filter is applied by subtracting a binomial filter of the order of 1000, corresponding to Gaussian smoothing with $\sigma = 22$ (in channels). Remaining broad band structures are removed by fitting and subtracting a second order polynomial during the DOAS fit.

In order to correct for small uncertainties in the wavelength mapping, we use one set of shift and squeeze parameters for all references spectra. The latter are taken from: NO_2 (Voigt et al., 2002), Glyoxal (CHOCHO) (Volkamer et al., 2005), O_3 (Voigt et al., 2001), O_4 (Greenblatt et al., 1990) and H_2O (Hitran 2006, see Rothman et al., 2003). For the non-linear optimization DOASIS uses a Levenberg-Marquard fit and b-splines for interpolation. The reference spectra are treated with the same high pass filter. The spectral fit is applied for wavelengths ranging from 436.3 nm to 460.5 nm which includes several strong NO_2 absorption lines. The measured slant columns are converted to mixing ratios by dividing the slant columns by the total absorption length and the air density. Simultaneous pressure and temperature measurements are used for the air density calculation. A DOAS fit example of the LP-DOAS measurement is shown in Fig. 3 with NO_2 slant column density of $1.84 \times 10^{17} \pm 1.53 \times 10^{15}$ moles cm^{-2} with respect to volume mixing ratio of 19.23 ± 0.16 ppbv. Based on findings by Stutz and Platt (1996) the numerical error of the fit is multiplied by a factor of 3 to obtain an estimate of the measurement error. The detection limit is defined by 2 times this measurement error (Stutz and Platt, 1996). We compared this detection limit to an estimate gained from analyzing the higher frequency variations in our time series. The latter are assumed to be dominated by instrument noise as path averaged NO_2 concentrations should vary on larger time scales. Applying a high pass filter with a threshold of 10 min to the data of one day, we obtain a variance of the remaining high frequency structure of about 0.5 ppbv, which agrees well with the estimate of the measurement error from the DOAS evaluation. This value is considered to be the upper limit of the measurement error. Typically, the error of the NO_2 measurment is in the order of 1 % and thus ignoreable in the following discussions. Due to visuality the LP-DOAS measurement error is not plotted in the concentration time series.

3 Results

The LP-DOAS has been measuring for more than 16 months, providing atmospheric NO_2 information with high temporal resolution. The data show strong daily, weekly and seasonal variability. Mean daily cycles of NO_2 for weekday and Sunday show different characteristic. The typical daily cycle shows one peak in the morning and one peak in the evening rush hour. The lowest and highest NO_2 levels usually occur in the early morning and the evening rush hour, respectively. Details of the daily and weekly cycle of NO_2 will be discussed in Sect. 3.3. The annually averaged NO_2 concentration level measured by the LP-DOAS is about 23.5 ppbv, which is slightly higher than the WHO guideline annual value (21 ppbv), but considerably lower than the Hong Kong air quality annual objective value (42.5 ppbv). The maximum and minimum NO_2 concentration measured within the entire measuring period are 110.9 ppbv and 2.6 ppbv, respectively.

During this study, we also analyzed the relationship between NO_2 concentrations, wind direction and wind speed. In general, the NO_2 concentration is slightly higher when there are westerly winds, most likely due to transport from Hong Kong power plants. We could not observe a clear relation for wind from the industrial area in the Pearl River Delta NW of Hong Kong. This indicates that high NO_2 concentrations in Hong Kong do not arise from transport from these areas but have a local origin. We also find that the NO_2 concentrations decrease with increasing wind speed for all wind directions. Stronger winds prevent locally produced NO_2 from accumulating.

3.1 Comparison with in-situ monitoring data

In this section, we compare NO_2 measurements between the LP-DOAS and a nearby air quality monitoring station operated by the Hong Kong Environmental Protection Department (EPD) in Sham Shui Po about 1.6 km from our measuring site (http://www.epd-asg.gov.hk/english/backgd/quality.html). The monitoring station is located on top of the Sham Shui Po police station at about 17 m above ground. The monitoring instrument is a chemiluminescence analyzer with Molybdenum converter which measures atmospheric NO_2 by converting NO_2 to NO. Roadside measurements of another EPD station with the same type of instrument located in Mong Kok are given in the following as well. The location of both EPD stations are marked in Fig. 2.

Time series of daily averaged ambient NO_2 concentrations obtained by the LP-DOAS and the EPD monitoring station from December 2009 till March 2011 are shown in Fig. 4a. Figure 4b and c shows the EPD measurements and hourly averaged LP-DOAS measurements for the two setups, respectively. For the longer absorption path data from the EPD roadside monitoring station in Mong Kok are also shown. NO_2 concentrations show similar characteristic: both time series show a pronounced daily and annual cycle with lower NO_2 levels in summer. Higher photolysis rates and longer daylight hours convert more NO_2 to NO and O_3, and a higher precipitation rate increases the wet deposition rate of NO_2 resulting in lower NO_2 concentration levels.

Figure 5a shows that the Pearson correlation coefficient between the CityU LP-DOAS and Sham Shui Po EPD data set is 0.71, the regression line has a slope of 0.80 with an offset of 16.1 ppbv. On average the EPD monitor in Shum Shui Po measures concentrations that are 11.5 ppbv higher than the LP-DOAS. This might be explained by the difference in the environment of the measuring sites. The EPD monitoring station is located in Sham Shui Po, a commercial area with heavy traffic, while the LP-DOAS instrument was set up in Kowloon Tong with the absorption path covering the University Campus and residential area.

Figure 5b indicates the Pearson correlation coefficient between the LP-DOAS with path from CityU to Langham Place Hotel and EPD measurements in Sham Shui Po is 0.79, decreasing to 0.62 for the correlation between the LP-DOAS and Mong Kok EPD roadside measurements. On average the Sham Shui Po and Mong Kok EPD values are 15.6 ppbv and 40.7 ppbv higher than the LP-DOAS. Measured concentrations decreasing with increasing measurement height suggests that the main emission sources and formation of NO_2 are very close to the ground and probably dominated by traffic emissions. This result agrees with the observation that the EPD roadside monitoring stations typically measure higher NO_2 concentrations than the average station (Lau et al., 2008).

Figure 4 illustrates that most of the time the NO_2 concentrations recorded by the EPD monitoring station correlate well with the LP-DOAS measurements. However, the EPD monitoring station measurements occasionally show a considerable disagreement compared to the LP-DOAS measurements (e.g. Fig. 4b 28 February and 3 March 2010). This phenomenon can be explained by the differences in the measuring technique: the LP-DOAS remote sensing measures atmospheric NO_2 without influencing the concentrations and without any cross sensitivity to other nitrogen species, whereas the chemiluminescence analyzing technique is reported to suffer from significant interference by other nitrogen compounds. The conversion of these compounds can lead to overestimation of the measured NO_2 concentration up to 50 % in heavily polluted urban areas like Hong Kong (Dunlea et al., 2007). Additionally, the chemiluminescence measurement is a point measurement, while the LP-DOAS measures the average NO_2 concentration along an absorption path. Therefore, the LP-DOAS is less influenced by a single emission and local fluctuations.

3.2 Satellite measurement validation

Satellite measurements of atmospheric trace gases are indispensable for providing global maps of trace gas distributions. However, there are very few satellite validation studies over South China. In order to find out how representative satellite derived NO_2 columns are for ground level concentrations in Hong Kong, we compare the LP-DOAS NO_2 data to OMI satellite measurements.

3.2.1 The ozone monitoring instrument

OMI is an imaging spectrometer measuring atmospheric trace gases such as NO_2 and O_3. It is on board the Earth Observing System's (EOS) Aura satellite which was launched on 15 July 2004 and is collecting data since 9 August 2004, providing more than 6 yr of daily global NO_2 maps (Boersma et al., 2001). The Aura satellite orbits at an altitude of 705 km in a sun-synchronous polar orbit with an exact 16 day repeat cycle and a local equator crossing time of 13:45 (local time) on the ascending node. The instrument consists of two nadir viewing imaging spectrometers measuring the UV/VIS spectral range from 264 nm to 504 nm with a spectral resolution between 0.45 nm and 1.0 nm FWHM. The spectral sampling is two to three times the spectral resolution. OMI provides measurements at 60 positions across the orbital track every 2 s. In the global observation mode, these 60 measurements cover a swath of approximately 2600 km. The ground pixel size of OMI at nadir is about 320 km^2 (13 km × 24 km) and increases to about 6400 km^2 (40 km × 160 km) at the two ends of the track. The change in ground pixel size, and hence spatial resolution, must be taken into account when analyzing and interpreting OMI data. A more detailed description of the OMI instrument can be found in Levelt et al. (2006).

3.2.2 OMI tropospheric NO_2 VCD retrieval

In this study, NASA's OMI tropospheric NO_2 data product is used. The NO_2 slant column density (SCD) is retrieved by fitting the OMI spectrum for wavelengths ranging from 405 nm to 465 nm using the DOAS technique. For the OMI NO_2 data product three trace gas reference spectra, NO_2 (Vandaele et al., 1998), O_3 (Burrows et al., 1999) and H_2O (Harder and Brault, 1997), are fitted to the measured spectra. The air-mass factor (AMF), defined as the ratio of the SCD to the vertical column density (VCD), is needed in order to convert SCD into VCD (Solomon et al., 1987). The AMF calculation depends on the viewing geometry, surface albedo, atmospheric scattering and the NO_2 vertical profile (Palmer et al., 2001). AMFs are calculated on the basis of annual mean NO_2 profiles obtained from the GEOS-Chem model (Bey et al., 2001) and pre-calculated altitude-dependent AMFs (Bucsela et al., 2006). The stratospheric and tropospheric amounts of NO_2 are separated by assuming the tropospheric NO_2 varies on a much smaller spatial scale than the stratospheric NO_2. Polluted regions are masked and the remaining stratospheric field is smoothed and interpolated using a zonal planetary wave analysis. This smoothed field is subtracted from the VCDs in order to calculate the tropospheric NO_2 amount by applying a corrected tropospheric AMF. For cloud contaminated pixels profiles are extrapolated to the ground (Bucsela et al., 2006).

3.2.3 Gridded OMI NO_2 data

Since there might be multiple OMI pixels overlapping each other, the OMI tropospheric NO_2 VCDs are gridded onto a high resolution longitude-latitude grid, in order to have a better comparison between the OMI NO_2 and the LP-DOAS measurements. For the comparison a $0.02^\circ \times 0.02^\circ$ grid (approximately 2.22 km × 2.05 km for Hong Kong) is used. The gridded product is based on all VCDs observed within a day for cloud cover less than 40 %. For overlapping OMI pixels a weighted average is stored in the grid cell. Weighting the VCDs with a factor $1/\mathrm{VCD}_{\mathrm{err}}^2$ would minimize the resulting average errors. However, the AMF calculation constitutes the largest error source, which leads to the NO_2 VCD uncertainties being proportional to the VCDs. Weighting with $1/\mathrm{VCD}_{\mathrm{err}}^2$ yields an average bias toward low VCD values. Following the approach introduced by Wenig et al. (2008), we adopt a weighting scheme which only depends on the error caused by the cloud cover C and the OMI pixel size A for the calculation of $\mathrm{VCD}_{\mathrm{GRID}}$

$$\mathrm{VCD}_{\mathrm{GRID}} = \frac{\Sigma \mathrm{VCD} \times W}{\Sigma W} \text{ with } W = \frac{1}{A(1.5 \times 10^{15}(1+3C))^2} \tag{1}$$

This gridding scheme can also enhance the details in the gridded product by giving smaller OMI pixels higher weight (Wenig et al., 2008).

3.2.4 Converting tropospheric VCD to ground level concentration

The OMI tropospheric NO_2 VCDs are converted to ground level NO_2 mixing ratios using an annual mean vertical NO_2 profile (from July 2009 till June 2010) derived from a GEOS-Chem NOx-Ox-hydrocarbon-aerosol simulation. GEOS-Chem is a global 3-D chemical transport model (CTM) using meteorological input from the Goddard Earth Observing System (GEOS-5) of the NASA Global Modelling and Assimilation Office (GMAO) (Bey et al., 2001). It has a horizontal resolution of 2° (latitude) × 2.5° (longitude) and 47 hybrid pressure-eta levels. The GEOS-Chem grid cell containing Hong Kong also covers a large fraction of ocean and hence underestimates the ground level NO_2 concentration. To compensate for this, we computed a NO_2 profile by averaging the annual profile data of four grid cells surrounding Hong Kong (see Fig. 7) which includes the NO_2 plume over the Pearl River Delta region and used the resulting profile (see Fig. 6) to convert OMI NO_2 VCDs to ground mixing ratios.

3.2.5 Cloud filtering

Clouds shield ground level NO_2 and make satellite measurements difficult. In order to allow better comparison with the LP-DOAS data, OMI measurements significantly influenced by clouds have to be filtered out. To get a balance between having enough measurements left and minimizing cloud contamination, only OMI data with cloud fractions smaller than 40 % are used in this study. LP-DOAS data from 13:30 to 14:30 local time (which is the OMI overpass time for Hong Kong and hence is expected to have the best agreement with OMI data) are used for comparison with the gridded OMI data sets within 15 km from the measurement site (which is approximately the average OMI pixel size over Hong Kong), see Fig. 7. OMI data within 50vkm are shown for illustrations as well. In order to reduce the influence of clouds and local spatial variations, monthly mean data are used for the comparison.

3.2.6 Comparison of monthly values

Figure 8 shows the monthly averaged LP-DOAS data for the OMI overpass time from 13:30 to 14:30 and the OMI data converted to ground concentrations within a 15 km radius of CityU. Both data sets (LP-DOAS and OMI) show a very similar annual cycle with lower NO_2 values in summer and higher NO_2 values in autumn and winter. The Pearson correlation between the LP-DOAS measurements and OMI data within 15 km is 0.84. In order to show the influence of temporal averaging, monthly averages for all LP-DOAS data are shown in Fig. 8, too. As NO_2 shows high temporal variability, increasing the averaging time would include data that OMI is not able to capture and hence less correlated with each other. OMI data averaged for a 50 km radius illustrates the influence of spatial averaging. As can be seen in Fig. 7, Hong Kong is at the edge of the NO_2 plume covering the entire Pearl River Delta which means increasing the averaging area to increase spatial coverage would include other, more dominant sources not related to local emissions measured by the LP-DOAS. This agrees with the fact that the correlation coefficient decreases to 0.64 for the corresponding data sets. On average the monthly means of the OMI data within 15 km and 50 km are lower than the LP-DOAS measurement by 6.32 ppbv and 10.39 ppbv, respectively.

The error bars shown in Fig. 8 representing the 1σ uncertainties of the OMI data. The errors of the monthly OMI data are calculated by the standard error propagation and base on the assumption that all errors are randomly distributed. The error bars are larger for the months when only a small number of data points were available due to cloud filtering, e.g. February, April and May of 2010. In most of the months, the error bars of OMI data, either within 15 km or within 50 km, do not overlap with the LP-DOAS data, which indicated that there are some unknown systematic errors either in the OMI retrieval (Wenig et al., 2008) or the VCDs to ground level concentrations conversion, or both. Since this errors are purely systematic, and hence cannot be reduced by averaging. One possible reason for the lower OMI values over Hong Kong compared to the LP-DOAS measurements is that the average GEOS-Chem NO_2 vertical profile used in converting the tropospheric NO_2 VCDs to ground level concentrations is averaged over a large area around the Pearl River Delta Region including large fractions of ocean and rural area. As described in Sect. 3.2.4, we decided to use 4 GEOS-Chem cells covering the entire emission plume seen in Fig. 7 because the GEOS-Chem cell including Hong Kong contains mainly ocean pixels with an even lower relative ground level concentration. Underestimation of the relative ground level concentrations in the conversion profile leads to underestimation of the ground level NO_2 concentrations. Our findings are consistent with those of a similar comparison by Wenig et al. (2008).

3.3 Daily and weekly cycle of NO_2

Figure 9 shows the normalized mean weekly cycle of NO_2 for Hong Kong measured by the LP-DOAS and OMI. For each day of the week we calculated the mean of the LP-DOAS measurements and the OMI observations (cloud filtered) for the entire LP-DOAS measurment period from December 2009 to March 2011. LP-DOAS data are temporal averages around OMI overpass time (13:30 to 14:30), OMI data are spatial averages within 15 km and 50 km. Temporal averages of the LP-DOAS data around the morning rush hour (08:30 to 09:30) and daily mean are shown for reference. Both datasets are normalized by the mean weekday (Monday to Friday) value for better comparison, and to emphasize the relative reduction of NO_2 concentration on Sunday.

The OMI data and LP-DOAS data during OMI overpass agree with each other and show no significant weekly cycle. However, such a cycle can be observed in the LP-DOAS data during the morning rush hour (08:30 to 09:30). The weekly cycle shows that the NO_2 level reduces by more than 30 % on Sundays compared to weekdays.

The mean daily cycles of NO_2 concentrations for weekday, Saturday and Sunday are shown in Fig. 10. In general, NO_2 concentrations reach a minimum around 5:00 (local time) in the morning, followed by an increase from 5:00 to 9:00. The NO_2 concentration level decreases from 9:00 to 13:00 then it increases again and reaches the daily maximum around 18:00. The two peaks in the morning and the evening are due to an increase in traffic load during rush hours. Less traffic emissions and strong irradiance converting NO_2 to NO and ozone result in lower NO_2 concentrations at noon. Since natural and anthropogenic non-transportation NO_2 emissions have no weekly and diurnal cycle, we can conclude that the measured NO_2 are mainly due to traffic emissions.

From Fig. 10 it is obvious that the daily NO_2 cycle for weekdays and Saturdays are almost the same. Most of the people in Hong Kong have to work on Saturdays, hence the traffic volume on Saturday is similar to that of weekdays. The NO_2 concentration reduces significantly on Sunday morning by more than 30 % compared to weekdays. It gradually returns to a weekday level in the afternoon. This pattern might be be explained by the fact that the majority of the population does not have to work on Sunday and go out in the afternoon.

Similar to the noon LP-DOAS data, OMI NO_2 observations do not show any reduction on Sunday. However, the LP-DOAS data show a significant reduction on Sunday morning. This suggests that satellite data with a single overpass per day are not sufficient to interpret weekly cycles of components which show a strong daily variability.

4 Summary and conclusion

In this paper, we describe the instrumental setup and automatic data retrieval process of the LED based long path DOAS instrument running operationally at City University of Hong Kong since December 2009 in order to monitor surface air pollution conditions in Hong Kong. The measured NO_2 data show strong daily, weekly and seasonal variability. The annually averaged NO_2 concentration is 23.5 ppbv but regularly exceeds 42.5 ppbv (Hong Kong air quality annual objective value). The NO_2 concentrations vary from 2.6 ppbv to 110.9 ppbv during the entire measuring period.

Our LP-DOAS measurements are compared to the concentration reported by a nearby monitoring station operated by the Hong Kong Environmental Protection Department (EPD). Hourly averages of coinciding measurements correlate well with a correlation coefficient $R = 0.71$ for the 550 m absorption path and 0.79 for the 3820 m path. However, the EPD measurements show higher NO_2 concentrations than the LP-DOAS measurements by 11.5 ppbv for the shorter path and 15.6 ppbv for the longer path. This discrepancy can be explained by different measurement heights and locations. Previous study reported that the chemiluminescence analyzers are likely to be overestimating the NO_2 concentrations due to cross interferences from other nitrogen compounds.

The LP-DOAS measurements during the OMI overpass time (13:30–14:30) are used to validate OMI satellite NO_2 measurements over Hong Kong. Monthly averaged data of the LP-DOAS and OMI within 15 km radius of the LP-DOAS correlate well with a correlation coefficient of 0.84 and show that OMI measures reliable ground level NO_2 concentrations. However, the OMI data are on average 5.45 ppbv (22 %) lower than the LP-DOAS measurements. This discrepancy might due to the NO_2 vertical profile used for the conversion of OMI NO_2 VCDs to ground level concentrations.

Weekly cycles from OMI data and LP-DOAS data show clear differences. Daily NO_2 cycles from LP-DOAS measurements show significant peaks in the morning and evening rush hour due to increased traffic. The weekly cycle of NO_2 shows significant reduction on Sunday morning, but a typical weekday level for the rest of the day. This explains why OMI cannot observe a weekly cycle for Hong Kong, since the satellite's overpass time is around 14:00. We demonstrate that satellite data with a single overpass per day are not in general suitable to derive weekly cycles of compounds with strong diurnal variation.

Acknowledgements. The authors would like to thank the Langham Place Hotel for cooperating with CityU on this project and for the installation of the retro reflector at their building. The work described in this paper was partial supported by a grant from the Research Grants Council of the Hong Kong Special Administrative Region, China (Project No. CityU 102809), a grant from City University of Hong Kong (Project No. 7008077) and the German DAAD (Project No. PPP-D/09/00817).

References

Bey, I., Jacob, D., Yantosca, R., Logan, J., Field, B., Fiore, A., Li, Q., Liu, H., Mickley, L., and Schultz, M.: Global modeling of tropospheric chemistry with assimilated meteorology: Model description and evaluation, J. Geophys. Res., 106, 23073, doi:10.1029/2001JD000807, 2001. 6624, 6625

Boersma, K. F., Bucsela, E. J., Brinksma, E. J., and Gleason, J. F.: NO_2, OMI-EOS Algorithm Theoretical Basis Document: Trace Gas Algorithms: NO_2, 2001. 6623

Bucsela, E., Celarier, E., Wenig, M., Gleason, J., Veefkind, P., Boersma, K., and Brinksma, E.: Algorithm for NO_2 vertical column retrieval from the Ozone Monitoring Instrument, IEEE T. Geosci. Remote Sens., 44, 1245–1258, 2006. 6624

Burrows, J. P., Richter, A., Dehn, A., Deters, B., Himmelmann, S., Voigt, S., and Orphal, J.: Atmospheric remote sensing reference data from GOME 2 Temperature-dependent absorption cross-sections of O_3 in the 231 V 794 nm range, J. Quant. Spectrosc. Ra., 61, 509–517, 1999. 6624

Crutzen, P.: The influence of nitrogen oxides on the atmospheric ozone content, Q. J. Roy. Meteorol. Soc., 96, 320–325, 1970. 6616

Dunlea, E. J., Herndon, S. C., Nelson, D. D., Volkamer, R. M., San Martini, F., Sheehy, P. M., Zahniser, M. S., Shorter, J. H., Wormhoudt, J. C., Lamb, B. K., Allwine, E. J., Gaffney, J.

S., Marley, N. A., Grutter, M., Marquez, C., Blanco, S., Cardenas, B., Retama, A., Ramos Villegas, C. R., Kolb, C. E., Molina, L. T., and Molina, M. J.: Evaluation of nitrogen dioxide chemiluminescence monitors in a polluted urban environment, Atmos. Chem. Phys., 7, 2691–2704, doi:10.5194/acp-7-2691-2007, 2007. 6622

Greenblatt, G., Orlando, J., Burkholder, J., and Ravishankara, A.: Absorption measurements of oxygen between 330 and 1140 nm, J. Geophys. Res., 95, 18577–18582, 1990. 6619

Harder, J. W. and Brault, J. W.: Atmospheric measurements of water vapor in the 442nm region, J. Geophys. Res., 102, 6245–6252, 1997. 6624

Kraus, S.: DOASIS A Framework Design for DOAS, Ph.D. thesis, Combined Faculties for Mathematics and for Computer Science, University of Mannheim, 2005. 6619

Lau, J., Hung, W., Cheung, C., and Yuen, D.: Contributions of roadside vehicle emissions to general air quality in Hong Kong, Transportation Res. D, 13, 19–26, 2008. 6617, 6622

Lee, D. S., Köhler, I., Grobler, E., Rohrer, F., Sausen, R., Gallardo-Klenner, L., Olivier, J. G. J., Dentener, F. J., and Bouwman, A.: Estimations of Global NO_x Emissions and Their Uncertainties, Atmos. Environ., 31, 1735–1749, 1997. 6617

Levelt, P. F., van den Oord, G. H. J., Dobber, M. R., Malkki, A., Visser, H., de Vries, J., Stammes, P., Lundell, J. O. V., and Saari, H.: The Ozone Monitoring Instrument, IEEE T. Geosci. Remote Sens., 44, 1093–1101, 2006. 6623

Merten, A., Tschritter, J., and Platt, U.: New Design of DOAS-Long-path Telescopes based on fiber optics, Appl. Opt., 50, 783–754, 2011. 6618

Palmer, P., Jacob, D., Chance, K., Martin, R., Spurr, R., Kurosu, T., I. Bey, R. Y., and Fiore, A.: Air mass factor formulation for spectroscopic measurements from satellites: Application to formaldehyde retrievals from the Global Ozone Monitoring Experiment, J. Geophys. Res., 106, 14539–14550, 2001. 6624

Platt, U., Perner, D., and Patz, H.: Simultaneous measurement of atmospheric CH_2O, O_3 and NO_2 by differential optical absorption, J. Geophys. Res., 84, 6329–6335, 1979. 6617

Rothman, L., Barbe, A., Benner, D. C., Brown, L., Camy-Peyret, C., Carleer, M., Chance, K., Clerbaux, C., Dana, V., Devi, V., Fayt, A., Flaud, J.-M., Gamache, R., Goldman, A., Jacquemart, D., Jucks, K., Lafferty, W., Mandin, J.-Y., Massie, S., Nemtchinov, V., Newnham, D., Perrin, A., Rinsland, C., Schroeder, J., Smith, K., Smith, M., Tang, K., Toth, R., Auwera, J. V., Varanasi, P., and Yoshino, K.: The HITRAN molecular spectroscopic database: edition of 2000 including updates through 2001, J. Quant. Spectrosc. Ra., 82, 5–44, 2003. 6619

Solomon, S., Schmeltekopf, A. L., and Sanders, R. W.: On the interpretation of zenith sky measurements, J. Geophys. Res., 92, 8311–8319, 1987. 6624

Solomon, S., Portmann, R. W., Sanders, R. W., Daniel, J. S., Madsen, W., Bartram, B., and Dutton, E. G.: On the role of nitrogen dioxide in the absorption of solar radiation, J. Geophys. Res., 104, 12047–12058, 1999. 6617

Stutz, J. and Platt, U.: Numerical Analysis and Estimation of the Statistical Error of Differential Optical Absorption Spectroscopy Measurements with Least-Squares methods, Appl. Opt., 35, 6041–6053, 1996. 6620

Stutz, J. and Platt, U.: Improving longpath differential optical absorption spectroscopy with a quartz-fiber mode mixer, Appl. Opt., 36, 1105–1115, 1997. 6618

Vandaele, A. C., Hermans, C., Simon, P. C., Carleer, M., Colin, R., Fally, S., Merienne, M. F., Jenouvrier, A., and Coquart, B.: Measurements of the NO_2 absorption cross-section from 42000 cm^{-1} to 10000 cm^{-1} (238–1000 nm) at 220 K and 294 K, J. Quant. Spectrosc. Ra., 59, 171–184, 1998. 6624

Voigt, S., Orphal, J., Bogumil, K., and Burrows, J. P.: The temperature dependence (203-293 K) of the absorption cross sections of O_3 in the 230–850 nm region measured by Fourier-transform spectroscopy, J. Photochem. Photobiol., 143, 1–9, 2001. 6619

Voigt, S., Orphal, J., and Burrows, J. P.: The temperature and pressure dependence of the absorption cross-sections of NO_2 in the 250-800 nm region measured by Fourier-transform spectroscopy, J. Photochem. Photobiol., 149, 1–7, 2002. 6619

Volkamer, R., Spietz, P., Burrows, J., and Platt, U.: High-resolution absorption cross-section of Glyoxal in the UV/vis and IR spectral ranges, J. Photochem. Photobiol., 172, 35, doi:10.1016/j.jphotochem.2004.11.011, 2005. 6619

Wenig, M. O., Cede, A. M., Bucsela, E. J., Celarier, E. A., Boersma, K. F., Veefkind, J. P., Brinksma, E. J., Gleason, J. F., and Herman, J. R.: Validation of OMI tropospheric NO_2 column densities using direct-sun mode Brewer measurements at NASA Goddard Space Flight Center, J. Geophys. Res., 133, D16S45, doi:10.1029/2007JD008 988, 2008. 6625, 6627

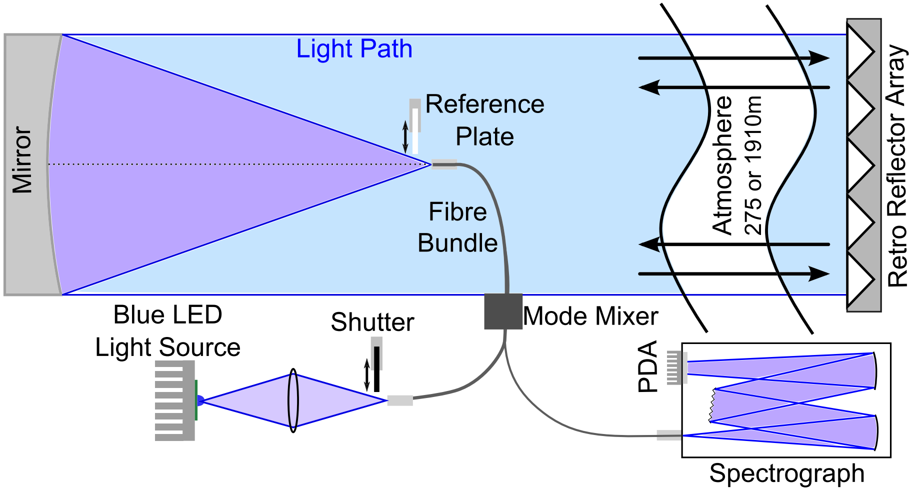

Fig. 1. Schematic diagram of the experimental setup of the fibre LP-DOAS.

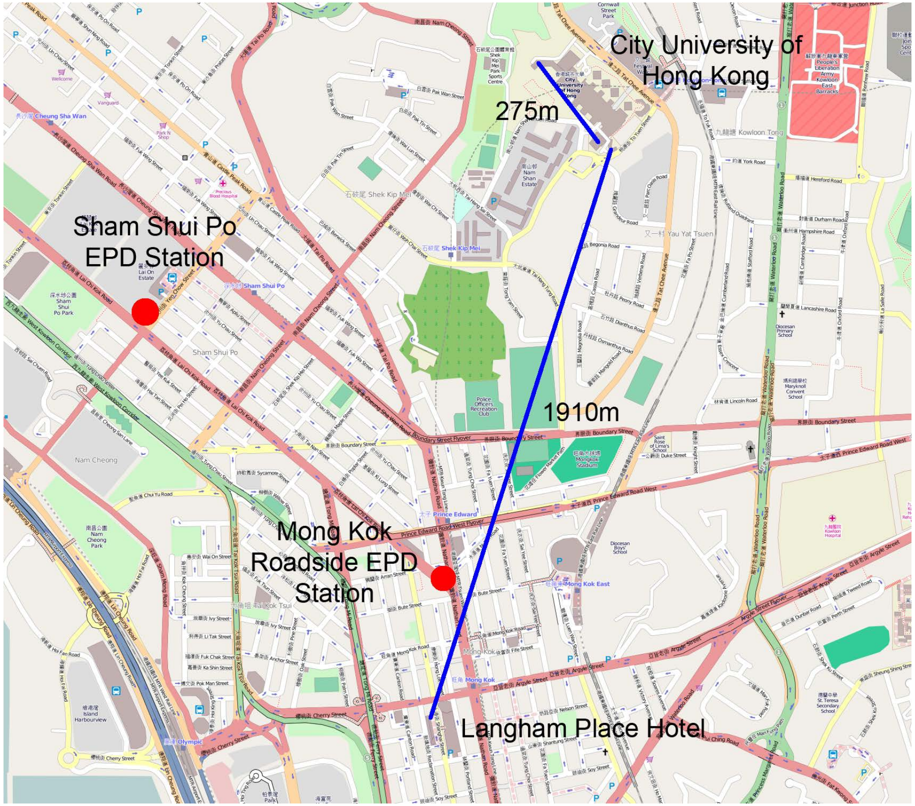

Fig. 2. Map of Kowloon, Hong Kong, from Open Street Map (http://www.openstreetmap.org) . The two blue lines indicate the measuring path for the two setups. The two red markers indicate the location of the Shum Shui Po and Mong Kok EPD monitoring station.

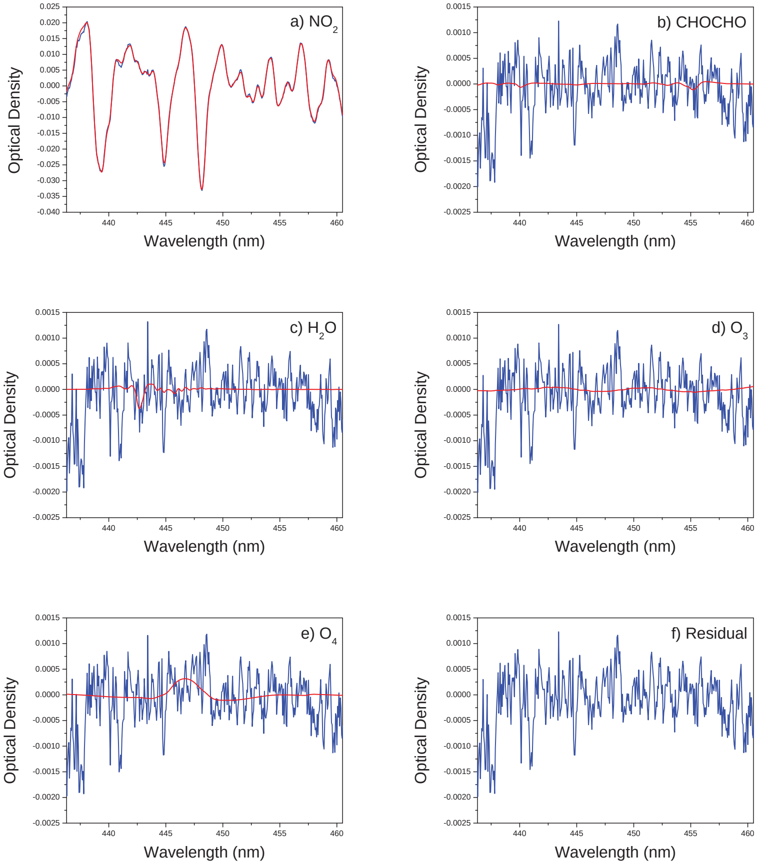

Fig. 3. Example of the NO$_2$ retrieval form a spectrum taken on 17 December 2010 at 09:54 (HKT). The optical density of the scaled cross-sections (red curves) and the sum of the scaled cross-section and the residual (blue curves) of (**a**) NO$_2$, (**b**) CHOCHO, (**c**) H$_2$O, (**d**) O$_3$ and (**e**) O$_4$. (**f**) shows the residual.

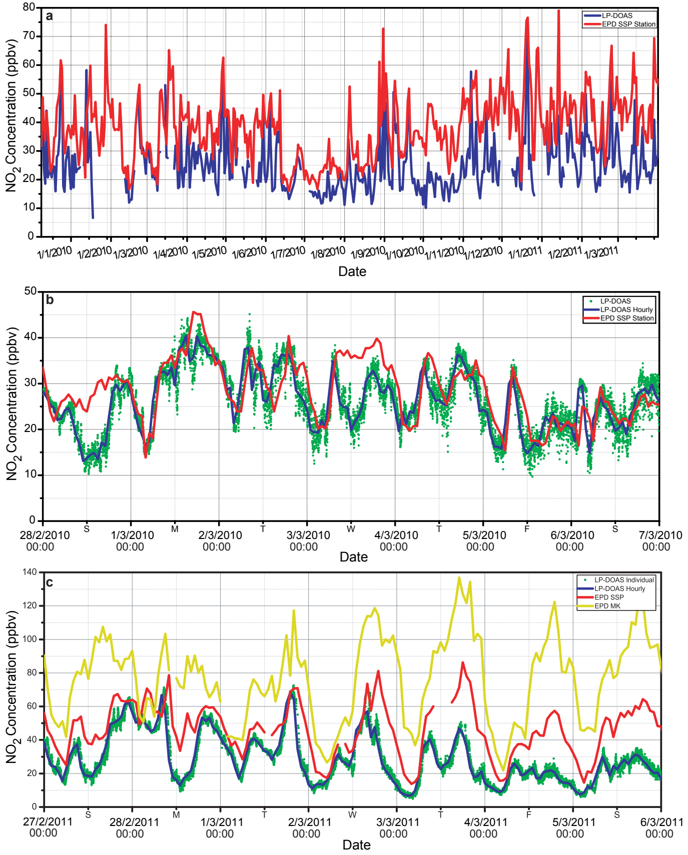

Fig. 4. Atmospheric NO$_2$ concentration measured by LP-DOAS at CityU and EPD Sham Shui Po monitoring station. (**a**) Daily averaged data from December 2009 to March 2011, (**b**) and (**c**) NO$_2$ time series for the first week of March of 2010 and 2011, respectively.

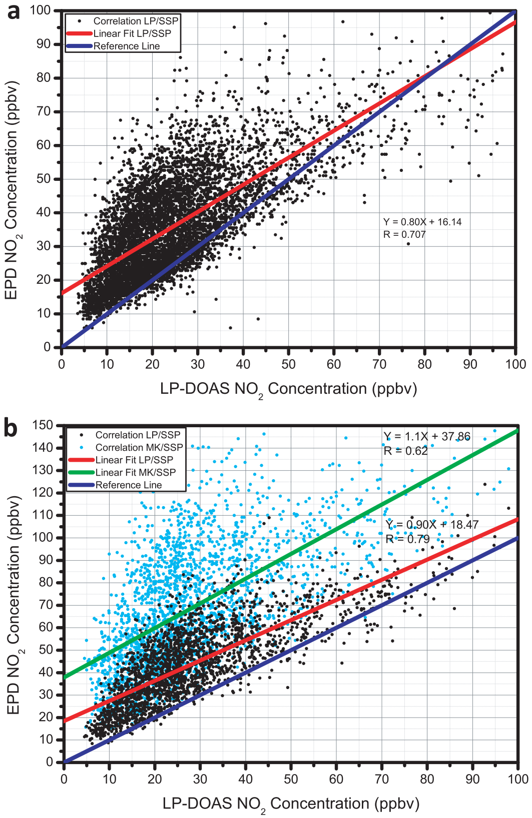

Fig. 5. (**a**) Correlation between concentrations measured by the LP-DOAS with CityU path (shorter path, x-axis) and the EPD Sham Shui Po monitoring station (y-axis), for data from December 2009 to November 2010. (**b**) Correlation between concentrations measured by the LP-DOAS with Langham Place path (longer path, x-axis) and the EPD Sham Shui Po (black dots) and Mong Kok (cyan dots) monitoring station (y-axis), for data from December 2010 to March 2011.

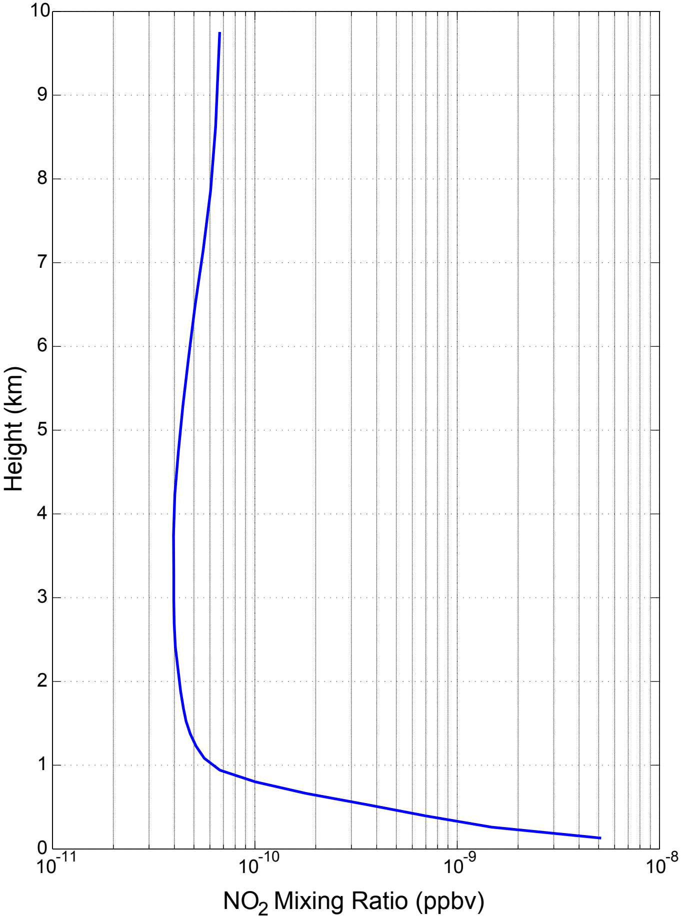

Fig. 6. Average vertical profile of NO_2 for the Pearl River Delta from GEOS Chem Model.

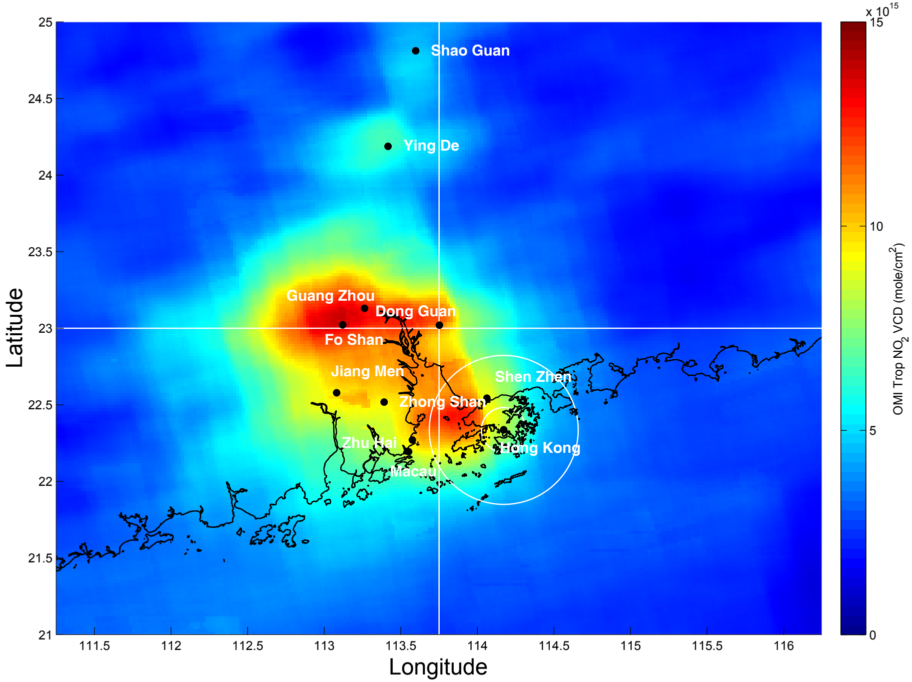

Fig. 7. Average OMI tropospheric NO_2 vertical column density gridded with a $0.02^\circ \times 0.02^\circ$ resolution over South China from December 2009 to March 2011. The two circles indicate the averaging area of the OMI data with Hong Kong in the centre. The four cells indicate the averaging area for the vertical profile calculation using GEOS-Chem.

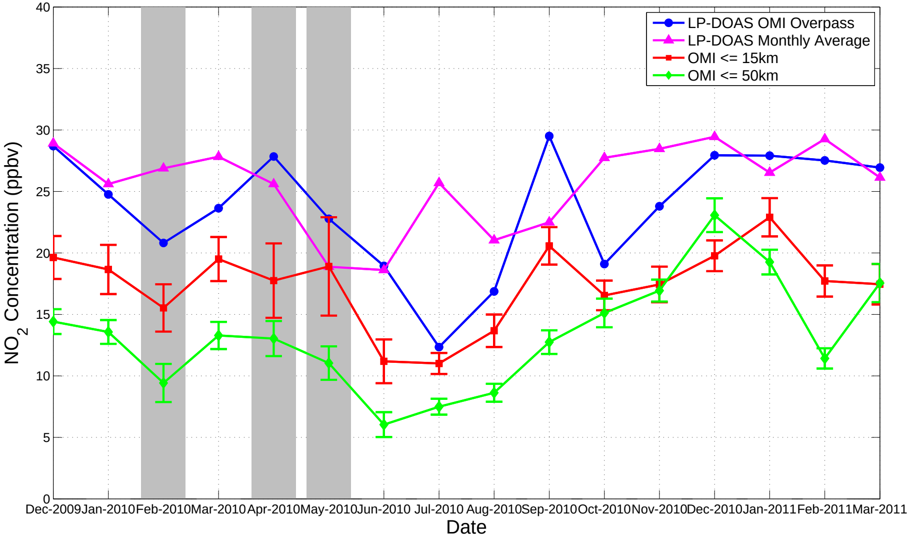

Fig. 8. Monthly mean ground level NO_2 concentration. LP-DOAS data are temporal averages around OMI overpass times (blue curve). Monthly averages for all LP-DOAS data is shown for reference (purple curve). The gray regions indicate months where OMI data are very sparse (less than 3 data points per month due to the cloud filtering). OMI data are spatial averages over pixels within a 15 km (red curve) and 50 km (green curve) radius of the instrument.

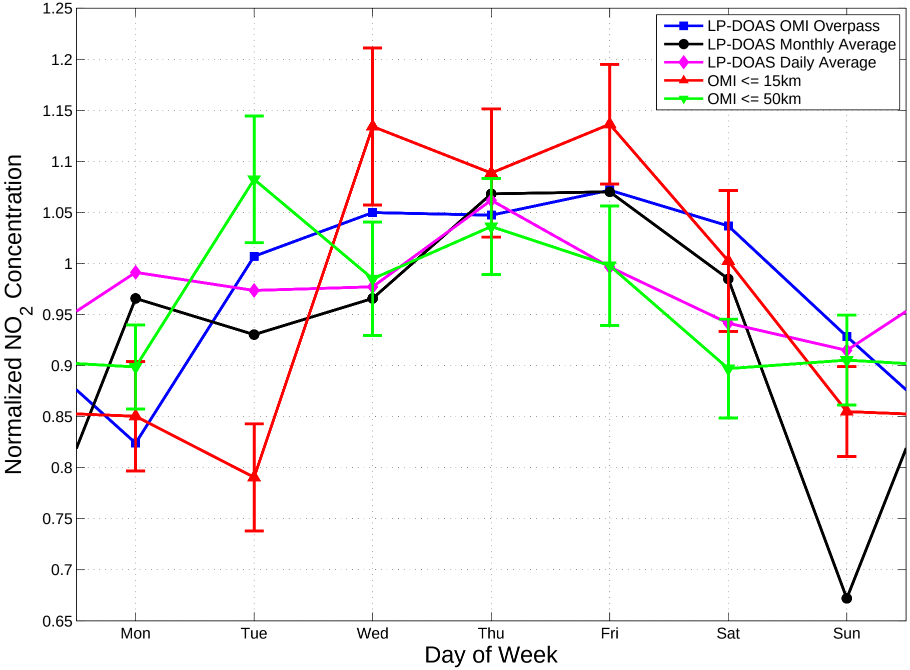

Fig. 9. Mean weekly cycle of NO_2 measured by OMI and LP-DOAS. The values are normalized with respect to the mean weekday (Monday to Friday) value (relative units). LP-DOAS data are temporal averages around OMI overpass time (blue curve) and around the morning rush hour (black curve), OMI data are spatial averages within 15 km (red curve) and 50km (green curve).

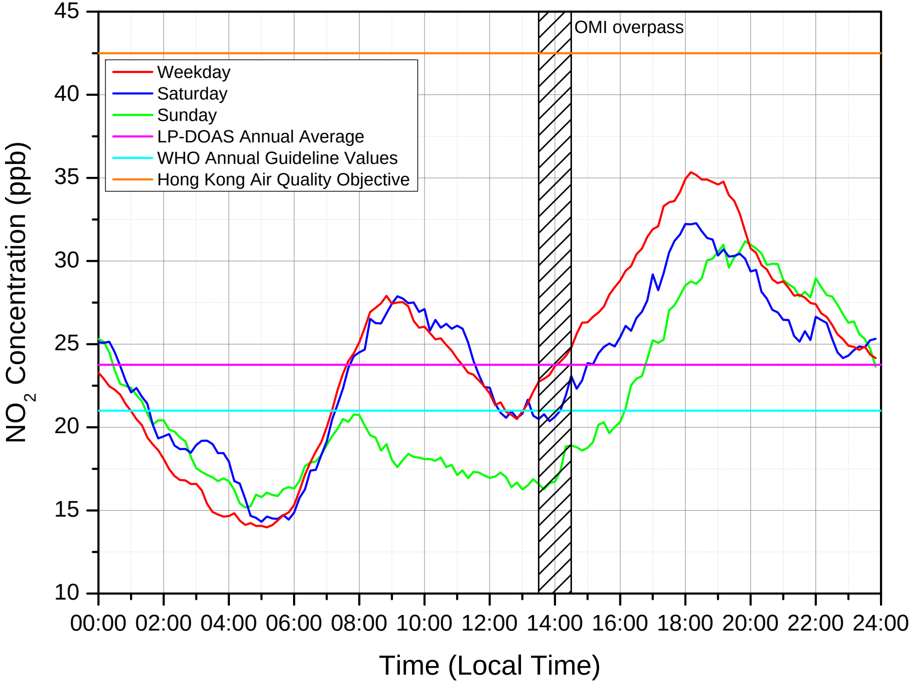

Fig. 10. Annual mean daily NO_2 cycle for weekday (red curve), Saturday (blue curve) and Sunday (green curve), for data from December 2009 to November 2010. Values for the annual mean (magenta curve), WHO guideline (cyan curve) and Hong Kong air quality annual objective (orange curve) are also shown for reference. The highlighted region indicates the OMI overpass time for Hong Kong.